Reprinted from

Eighth International Symposium

Machine Processing of

Remotely Sensed Data

with special emphasis on

Crop Inventory and Monitoring

July 7-9, 1982

Proceedings

Purdue University
The Laboratory for Applications of Remote Sensing
West Lafayette, Indiana 47907 USA

MONTE CARLO SIMULATIONS OF ATMOSPHERIC SPREADING FUNCTIONS FOR SPACE-BORNE OPTICAL SENSORS

RICHARD K. KIANG

National Aeronautics and Space Administration/Goddard Space Flight Center
New York, New York

I. ABSTRACT

A Monte Carlo radiative transfer model is used to simulate the atmospheric spreading effects. The spreading functions for several vertical aerosol profiles are obtained. The dependence of atmospheric conditions and aerosol properties are investigated, and the importance of the effect on MSS and TM measurements are assessed.

II. INTRODUCTION

It is a common experience to notice that well-defined features become blurred and hence less distinguishable from surroundings when viewed or photographed from a distance. This blurring phenomenum is due to the scattering of light by atmospheric constituents. In remote sensing of earth resources, the discrimination of ground types often solely relys on analyzing the radiance received at the sensors. But the received radiance includes the following two types of photons aside from those reflected from the ground target: (a) photons which never reach the ground but reflected by the atmosphere directly or indirectly back into the sensor, and (b) photons after having reached the area surrounding the target diffusely reflected back into the sensor. Superimposing on the signal, these photons blur the images acquired from space-borne platforms. In digital analyses, they distort the clusters and introduce additional deviations to the distributions. Consequently, pixels are misidentified and classification accuracy decreases. In scene simulation, ground or aircraft measurements are used to simulate satellite-received data. How to properly incorporate the influence of the background into the satellite observations is an important subject.

The atmospheric spreading effect is attributed to the second type of photons described above. In recent years, the influence of the background on satellite-received radiance have been investigated in several studies.[1-4] The spreading effect must be clearly understood to derive meaningful results from satellite observtaions, and to construct realistic simulated scenes.

In this paper, Section III describes the Monte Carlo method used to model the radiative transfer in the atmospheric-earth system, Section IV discusses the shapes of the atmospheric spreading functions for space-borne sensors, and how the shape varies with different vertical haze distributions. The spreading effects on MSS4 and TM2 observations are also investigated.

III. ATMOSPHERIC MODEL

The Monte Carlo method is used in this paper. Although numerical methods are available for solving radiative transfer problems, the Monte Carlo method remains the most flexible one in dealing with problems facing remote sensing of earth resources. In this paper, the general procedure outlined by House and Avery[5] are followed. In order to save computation time, backward photon tracing is used. The atmosphere is assumed non-absorbing. Hence a photon either escapes from the atmosphere or reaches the ground after successive collisions. Assuming a photon can only hit the ground once, then the spatial distributions of the photon population reaching the ground give the shapes of the unnormalized atmospheric spreading functions. The procedure used in this paper is described as follows. The atmosphere is divided into thirty-two layers. At the satellite a photon is released in the direction which the sensor

points to. After entering the atmosphere and travelling a distance, the photon may collide with either an air molecule or an aerosol, depending on their relative optical thickness in that layer. The distance that the photon travels before a collision occurs is determined by a logarithmic function. The direction the photon propagates after the collision is determined by the Rayleigh or the Mie phase function. In case the photon does not suffer any collision before leaving a layer, the distance it travels before a collision occurs in the next layer depends on the optical thickness of both layers. The above steps are repeated for each photon, until all the predetermined number of photons either escape from the atmosphere or collide with the ground.

The atmospheric spreading functions are the normalized population distributions on the ground for photons reflected by the ground and finally entering the satellite sensor. However, the ground-reflected radiance observed at the satellite is not just the convolution of the ground reflectance and the atmospheric spreading function. Due to the back-and-forth scatterings between the bottom of the atmosphere and the ground, the ground is not illuminated uniformly. The exact amount of solar irradiance falling on an area depends not only on the atmospheric condition but also on the target and the background reflectance.

The vertical pressure and temperature profiles for the 32-layer atmosphere are adopted from McClatchey et al.[6] The atmospheric spreading phenomenum highly depends on the vertical distributions of the Rayleigh and Mie optical thickness. The Rayleigh optical thickness profile may be computed from the pressure and the temperature profiles. The vertical optical thickness distribution for Mie scatterings are taken from LOWTRAN5.[7] To save computation time, the analytical Henyey-Greenstein phase function is used, with the asymmetry factor, g, set to 0.8. In each of the following examples, 10^4 photons of 0.55 μm are processed. This wavelength may be considered the band center of MSS4 and TM2.

IV. SIMULATION RESULTS

Figure 1 illustrates the atmospheric spreading function for a nadir-pointing sensor with an infinitesimal field-of-view. It has a very sharp center peak, and two wings extending to infinity. Surface area hundreds of kilometers away from the target may indeed contribute to the satellite-received radiance, but the contribution is so small that it may be ignored.

The spreading functions for MSS4 is shown in Figure 2 and Figure 3 in pixel resolution at a view angle of 2.89 degrees, for 50 km and 23 km meteorological range (aerosol optical thickness τ_{ao} = 0.16 and 0.32) respectively. The sharp center peaks are formed mainly by directly reflected photons. The two wings are formed by photons which are scattered at least once in reaching the sensor. As the aerosol optical thickness increases from 0.16 to 0.32, more collisions occur between photons and aerosols or air molecules. The center peak is lower, and the heights of the two wings increase. Thus background has a greater contribution to the satellite-received radiance. The two wings are not symmetrical except for a nadir-looking sensor. For a non-nadir looking sensor, the wing which the sensor points to has a smaller contribution.

The spreading functions for TM2 are shown in Figures 4 and 5 for midlatitude summer profile, with τ_{ao} = 0.16 and 0.32 respectively. The center peaks have the same heights as those in Figures 2 and 3, since the same set of τ_{ao} are used in both cases. But the background for TM2 is less concentrated toward the center than that for MSS4.

The contributions of the background pixels for MSS4 and TM2 are shown in Figure 6. The ordinate is the fraction of the total ground-reflected (by either target or background) radiance contributed by pixels summing outward from the target pixel. It is seen that at τ_{ao} = 0.16, the target contributes 82% of the ground reflected radiance, and at τ_{ao} = 0.32, the target contribution is 71%. As pointed out before, to include all the contributing background pixels is neither meaningful nor practical. An 85%-level or a 90%-level background may be a reasonable choice. The number of background pixels to either side of the target pixel which have to be included to achieve the 85% and 90% levels are summarized in Table 1.

Table 1.

	τ_{ao} = 0.16		τ_{ao} = 0.32	
	MSS4	TM2	MSS4	TM2
85%	3	6	12	23
90%	14	27	26	49

Figure 7 shows the fractions of the contributions to MSS4 for other haze profiles. It can be seen that the back-

ground areas has a smaller contribution in winter than in summer. And even a slightly volcanic upper atmosphere increases the contribution of the background significantly. For atmospheres with larger particulates, with g = 0.9, the number of background pixels to be considered is smaller. The fractions of contributions are given in Table 2.

Table 2.

	MSS4		
	τ_{ao}=0.18 summer volcanic	τ_{ao}=0.16 g=0.9	τ_{ao}=0.14 winter
85%	6	2	1
90%	25	8	8

V. DISCUSSIONS

It is shown above that as much as 20-30% of the ground reflected radiance originate from the background in a relatively clear (τ_{ao} = 0.16 - 0.32) atmosphere over a uniform ground. The atmospheric spreading function is sensitive to the aerosol loading, aerosol vertical distributions, and aerosol size. It is indicated that to account for 85% or 90% of the ground-reflected radiance, one has to consider anywhere from 1 to 25 pixels away from the target for MSS4, and approximately twice as many pixels for TM2.

Since it is impractical to consider the background in analyzing satellite data due to lack of either suitable model or precise atmospheric information, the contribution from the background is usually ignored. Excluding the path radiance, the background introduces 20-30% noise into the satellite data. Since spreading functions have very broad wings, how does the background noise vary over a relatively homogeneous landscape, such as a large agricultural area? Is it sufficiently uniform such that it is better not to perform background correction when atmospheric information is not precisely known? Or a partially corrected background effect is better than no correction? These are the questions that have to be answered in future studies.

REFERENCES

1. Pearce, W. A. 1977. A study of the atmosphere on Thematic Mapper observations. Report 004-77. EG&G, Washington Anal. Serv. Center, Appl. Sys. Dep., Riverdale, Maryland. 136pp.

2. Otterman, J., and R. S. Fraser. 1979. Adjacency effects on imaging by surface reflection and atmospheric scattering: cross radiance to zenith. Appl. Opt. 18:2852-2860.

3. Dave, J. V. 1980. Effect of atmospheric conditions on remote sensing of a surface nonhomogeneity. Photo. Eng. and Remote Sensing 46:1173-1180.

4. Kaufman, Y. J., and R. S. Fraser. 1981. The effect of finite field size on classification and atmospheric correction. NASA TM-83818, Goddard Space Flight Center, 48pp.

5. House, L. L., and L. W. Avery. 1969. The Monte Carlo technique applied to radiative transfer. J. Quant. Spectrosc. Radiat. Transfer 9:1579-1591.

6. McClatchey, R. A., et al. 1972. Optical properties of the atmosphere (third edition). AFCRL-72-0497. 108pp.

7. Kneizys, F. X., et al. 1980. Atmospheric transmittance/radiance: computer code LOWTRAN5. AFGL-TR-0067. 233pp.

Richard K. Kiang received the B.S. degree in physics from Cheng Kung University, Taiwan, and the Ph.D. degree in physics from the University of Michigan. From 1976 to 1980 he was the Earth Resources Manager of Sigma Data Corporation. Since 1980 he has been a Space Scientist at Institute for Space Studies, Goddard Space Flight Center. His professional interests include simulations of existing and future sensors, atmospheric effects on remotely sensed data, and classification techniques.

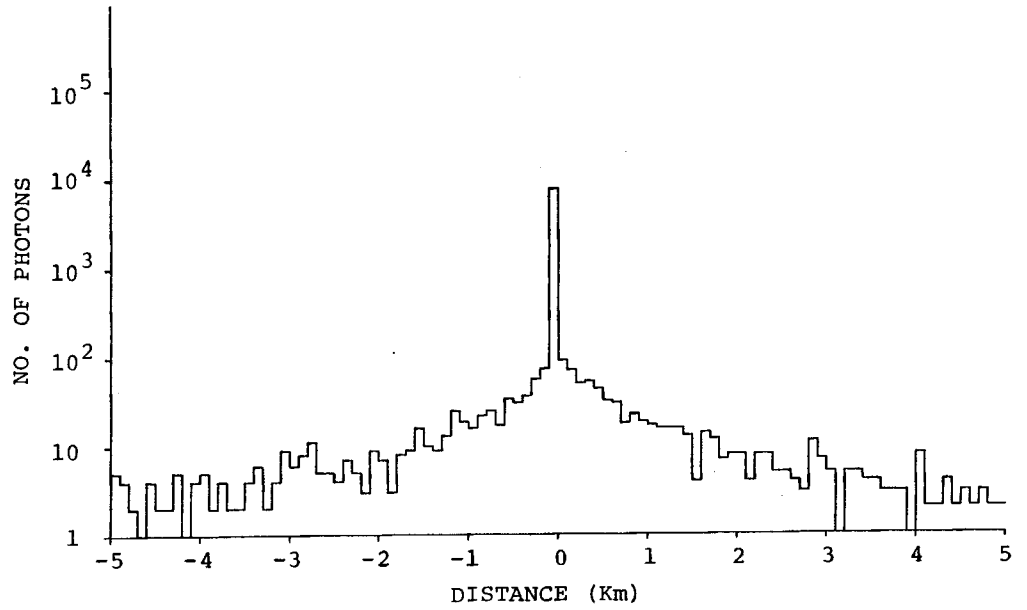

Fig. 1. Ground distribution of photon population for a space-borne sensor with infinitesimal field-of-view.

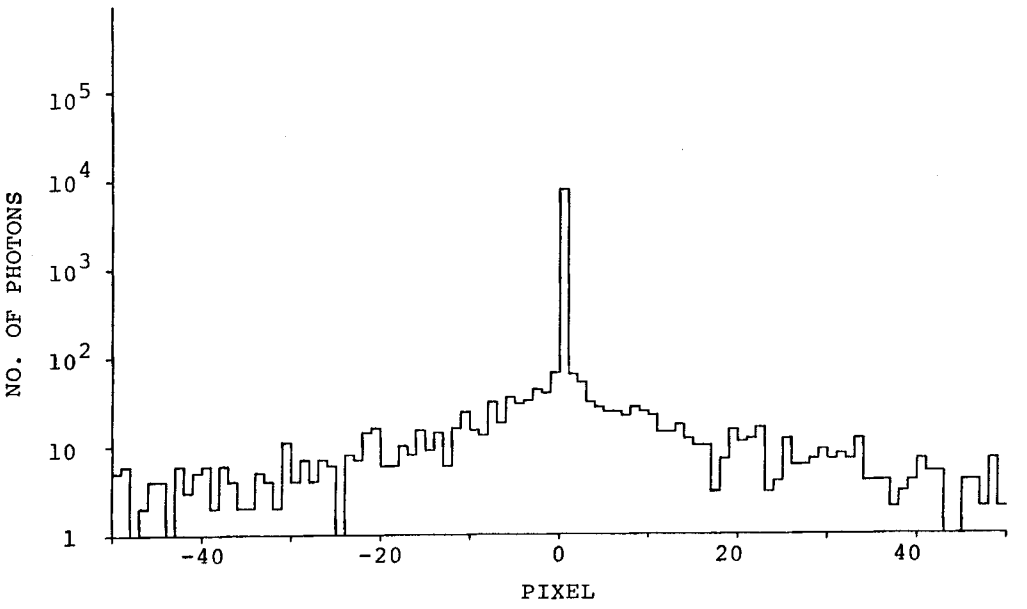

Fig. 2. Ground distribution of photon population for MSS4 at $\tau_{a0} = .16$.

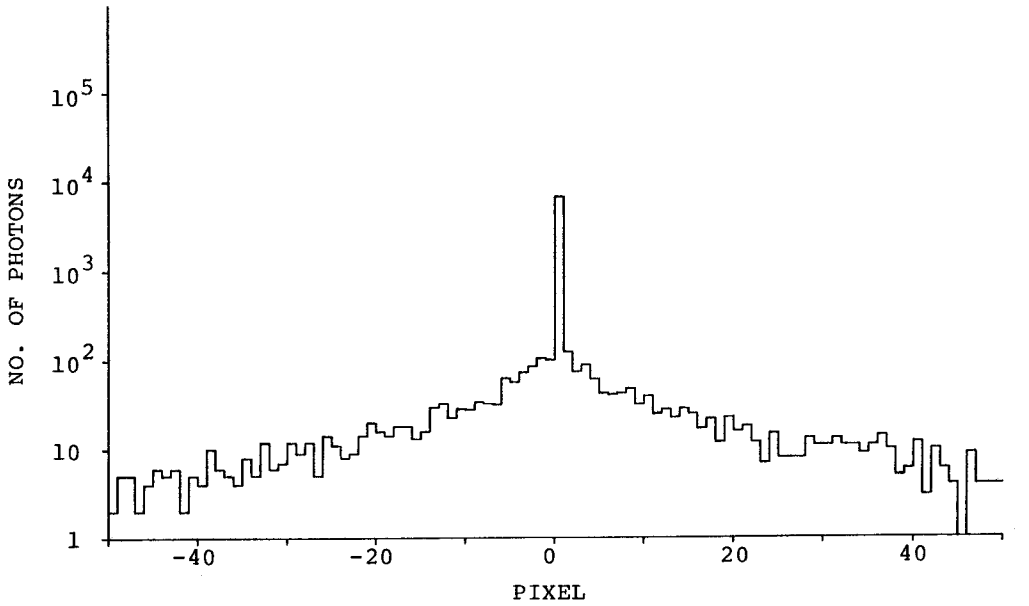

Fig. 3. Ground distribution of photon population for MSS4 at τ_{a0} = .32.

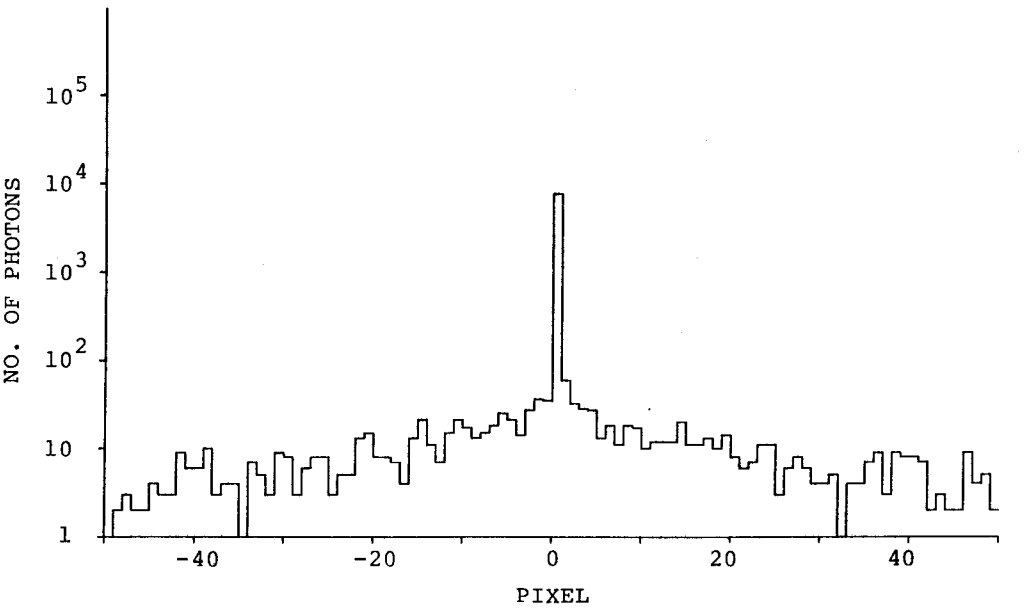

Fig. 4. Ground distribution of photon population for TM2 at τ_{a0} = .16.

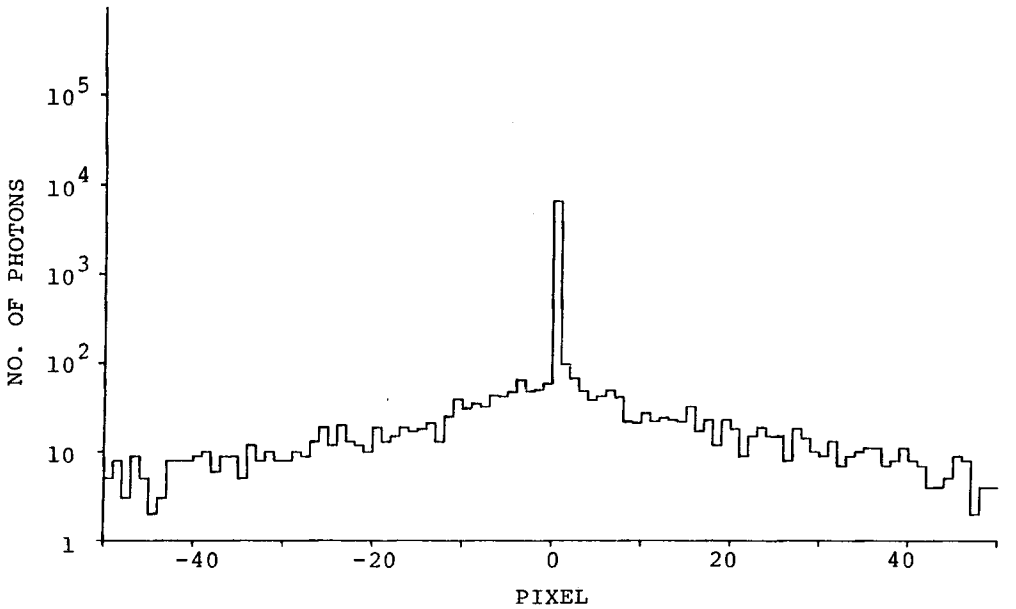

Fig. 5. Ground distribution of photon population for TM2 at τ_{a0} = .32.

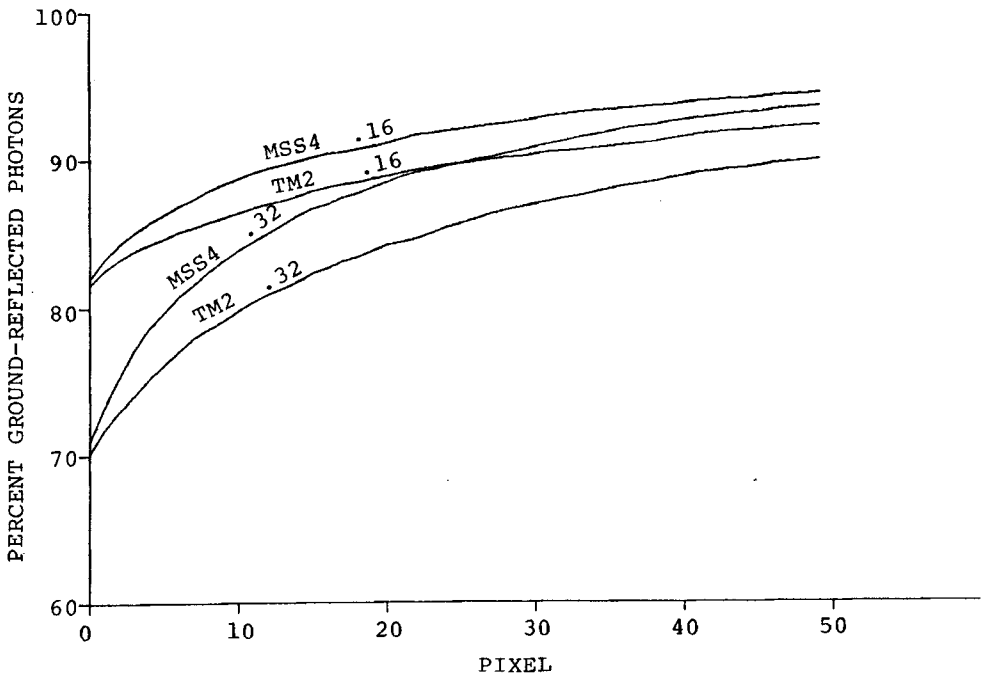

Fig. 6. Fractions of ground-reflected photons accumulated from target pixel, for MSS4 and TM2 at τ_{a0} = .16 and .32.

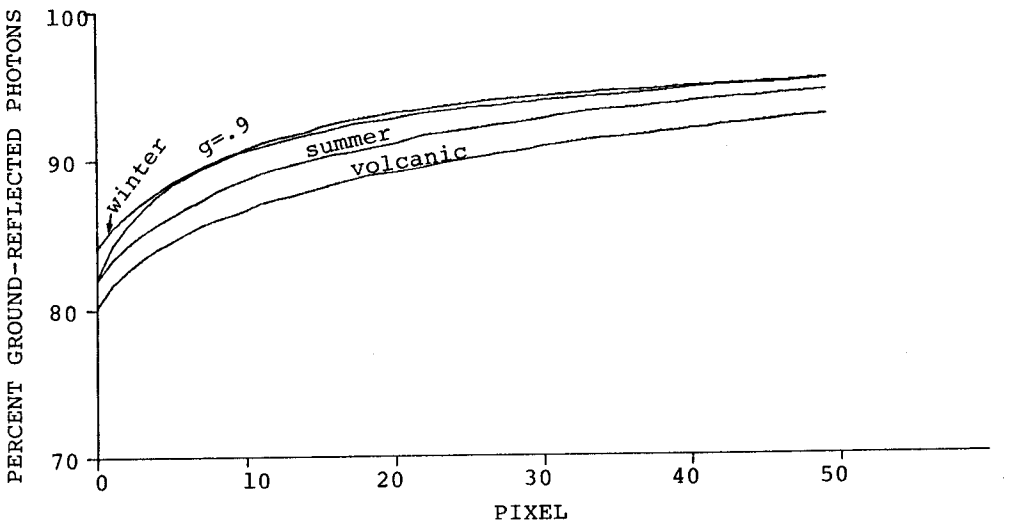

Fig. 7. Fractions of ground-reflected photons accumulated from target pixel for MSS4.